A peer-reviewed version of this preprint was published in PeerJ on 15 November 2016.

Sobeh M, ElHawary E, Peixoto H, Labib RM, Handoussa H, Swilam N, El-Khatib AH, Sharapov F, Mohamed T, Krstin S, Linscheid MW, Singab AN, Wink M, Ayoub N. 2016. Identification of phenolic secondary metabolites from *Schotia brachypetala* Sond. (Fabaceae) and demonstration of their antioxidant activities in *Caenorhabditis elegans*. PeerJ 4:e2404 https://doi.org/10.7717/peerj.2404

Identification of phenolic secondary metabolites from *Schotia brachypetala* Sond. (Fabaceae) and demonstration of their antioxidant activities in *Caenorhabditis elegans*

Mansour Sobeh, Esraa ElHawary, Herbenya Peixoto, Rola M Labib, Heba Handoussa, Noha Swilam, Ahmed A. El-Khatib, Farukh Sharapov, Tamer Mahmoud, Sonja Krstin, Michael Linscheid, Abdel Nasser Singab, Michael Wink, Nahla Ayoub

Background: *Schotia brachypetala* Sond. (Fabaceae) is an endemic tree of Southern Africa whose phytochemistry and pharmacology were slightly studied.The present work aimed at profiling the major phenolics compounds present in the hydro-alcoholic extract from *S. brachypetala* leaves (SBE) using LC/HRESI/MS/MS and NMR and prove their antioxidant capabilities using novel methods. **Methods:** In vitro assays; DPPH, TEAC persulfate decolorizing kinetic and FRAP assays, and in vivo assays: *Caenorhabditis elegans* strains maintenance, Intracellular ROS in *C. elegans,* Survival assay, GFP expression and Subcellular DAF-16 localization were employed to evaluate the antioxidant activity. **Results:** More than forty polyphenols ,including flavonoid glycosides, galloylated flavonoid glycosides, isoflavones, dihydrochalcones, procyanidins, anthocyanins, hydroxybenzoic acid derivatives, hydrolysable tannins, and traces of methylated and acetylated flavonoid derivatives were identified. Three compounds were isolated and identified from the genus *Schotia* for the first time, namely gallic acid, myricetin-3-*O*-*α*-L-$^{1}C_{4}$-rhamnoside and quercetin-3-*O*-L-$^{1}C_{4}$-rhamnoside.The tested extract was able to protect the worms against juglone induced oxidative stress and attenuate the reactive oxygen species (ROS) accumulation. SBE was also able to attenuate the levels of heat shock protein (HSP) expression. **Discussion:** A pronounced antioxidant activity *in vivo*, which can be attributed to its ability to promote the nuclear translocation of DAF-16/FOXO, the main transcription factor regulating the expression of stress response genes. The remarkable antioxidant activity *in vitro* and *in vivo* correlates to SBE rich phenolic profile.

Identification of phenolic secondary metabolites from *Schotiabrachypetala* Sond. (Fabaceae) and demonstration of their antioxidant activities in *Caenorhabditiselegans*

Sobeh, Mansour[a,], Esraa El-Hawary[b], HerbenyaPeixoto[a,], RolaLabib[b], Heba Handoussa[c], Noha Swilam[d], Ahmed H. El-Khatib[e,e'], FarukhSharapov[a], Tamer Mohamed[a], Sonja Krstin[a], Michael Linscheid[e], Abdel Nasser Singab[b], Michael Wink[a], NahlaAyoub[b, f*]

[a] Institute of Pharmacy and Molecular Biotechnology, Heidelberg University, ImNeuenheimer Feld 364, Heidelberg, Germany

[b] Department of Pharmacognosy, Faculty of Pharmacy, Ain Shams University, Cairo, Egypt

[c] Department of Pharmaceutical Biology, Faculty of Pharmacy, German University in Cairo, Egypt

[d] Department of Pharmacognosy, Faculty of Pharmacy, British University in Egypt, Cairo, Egypt.

[e] Department of Chemistry, Humboldt-Universität zu Berlin, Berlin, Germany

[e'] Pharmaceutical Analytical Chemistry Department, Faculty of pharmacy, Ain Shams University, Cairo, Egypt

[f] Department of Pharmacology and Toxicology, Faculty of medicine, Umm-AlQura University, Saudi Arabia.

***Author of Correspondence**

Prof. Dr.Nahla Ayoub

E-mail of correspondence: nahla.ayoub@yahoo.de

Telephone: 002-01223408226

Abstract

Background:*Schotiabrachypetala*Sond. (Fabaceae) is an endemic tree of Southern Africa whose phytochemistry and pharmacology were slightly studied.The present work aimed at profiling the major phenolics compounds present in the hydro-alcoholic extract from *S. brachypetala* leaves (SBE) using LC/HRESI/MS/MS and NMR and prove their antioxidant capabilities using novel methods.

Methods: In vitro assays; DPPH, TEAC persulfate decolorizing kinetic and FRAP assays, and in vivo assays: *Caenorhabditiselegans* strains maintenance, Intracellular ROS in *C. elegans,* Survival assay, GFP expression and Subcellular DAF-16 localizationwere employed to evaluate the antioxidant activity.

Results: More than forty polyphenols ,including flavonoid glycosides, galloylated flavonoid glycosides, isoflavones, dihydrochalcones, procyanidins, anthocyanins, hydroxybenzoic acid derivatives, hydrolysable tannins, and traces of methylated and acetylated flavonoid derivatives were identified. Three compounds were isolated and identified from the genus *Schotia* for the first time, namely gallic

acid, myricetin-3-*O*-*α*-L-$^{1}C_{4}$-rhamnoside and quercetin-3-*O*-L-$^{1}C_{4}$-rhamnoside.The tested extract was able to protect the worms against juglone induced oxidative stress and attenuate the reactive oxygen species (ROS) accumulation. SBE was also able to attenuate the levels of heat shock protein (HSP) expression.

Discussion:A pronounced antioxidant activity *in vivo*, which can be attributed to its ability to promote the nuclear translocation of DAF-16/FOXO, the main transcription factor regulating the expression of stress response genes. The remarkable antioxidant activity *in vitro* and *in vivo* correlates to SBE rich phenolic profile.

Key words:*Schotiabrachypetala,* polyphenolics, LC/HRESI/MS/MS, *Caenorhabditiselegans,* antioxidant activity.

Introduction

Plants produce a wide diversity of secondary metabolites, which have evolved as defence compounds against herbivores and microbes. Most secondary metabolites exhibit an interesting pharmacological activity. Therefore, many plants have been used in traditional medicine and phytomedicine for the treatment of health disorders all over the world (Wyk and Wink, 2004). In modern medicine, plants still have a special participation; anticancer compounds such as vinblastine, paclitaxel and camptothecin can be cited as enthusiastic examples of the pharmaceutical potential of the natural products (Efferth and Wink, 2010) Antiaging, antioxidants and anti-inflammatories are also currently found in natural source (Angerhofer, Maes&Giacomoni, 2008;Debnath, Kim& Lim, 2013;Kim et al., 2004; Yuan et al., 2006).

Antioxidants compounds are been extensively studied; they are supposed to play a role on aging and aging related diseases due to their ability to attenuate the cellular oxidative damage which are caused essentially by the reactive oxygen species (ROS) (Barja, 2004; Shaw, Werstuck& Chen, 2014).

The production of ROS is an inevitable result of the cell metabolism which can be enhanced by endogenous and exogenous stress. High concentrations of ROS cause oxidative damage on DNA, lipids and proteins; as a consequence, quite a number of health disorders are related to ROS intracellular imbalance, including arteriosclerosis and other cardio-vascular conditions, inflammation, cataract, Alzheimer's disease (Dumont &Beal., 2011; Pendergrass et al., 2006) and even cancer (Valko et al., 2004; Valko et al., 2007).

The cellular defence system against radicals include antioxidant enzymes, like superoxide dismutase, glutathione and catalase and compounds with antioxidant activity like proteins, vitamins, minerals and polyphenols (Sies& Stahl, 1995). ECGC and resveratrol are examples of polyphenols with potent antioxidant activity and demonstrated health benefits (Fujiki et al., 1999; Patel, et al., 2010; Rossi et al. 2008; Widlansky et al. 2007; Wolfram, 2007).

*Schotiabrachypetala*Sond. (Fabaceae), commonly named weeping boer-bean and huilboerbean (Afrikaans), is a tree endemic to southern Africa (Brenan, 1967; Watt &Breyer-Brandwijk, 1932). Polyhydroxystilbenes were isolated from the heartwood of the tree (Drewes& Fletcher, 1974) and two antibacterial fatty acids [methyl-5,11,14,17-eicosatetraenoate and 9,12,15-octadecatrienoic (δ-linolenic acid)] have been described from the leaves (McGaw, Jäger&Van Staden., 2002). Flavonolacylglucosides were recently reported from aerial parts of *S. brachypetala*(Du et al., 2014). A recent report indicates the presence of procyanidin isomers, quercetin 3-*O*rhamnoside, quercetin hexose gallic acid, quercetin hexose-protocatechuic acid, quercetin 3-*O* rhamnoside and ellagicacid in twigs (Hassaan et al., 2014). In addition, catechin and epicatechin have been isolated from plants of the genus *Schotia* (Masika, Sultana&Afolayan2004).

Traditional healers applied a decoction of the bark to strengthen the body and to treat dysentery and diarrhoea, nervous and heart conditions, flu symptoms and as an emetic. The roots are also used to treat diarrhoea and heartburn. The seeds can be roasted and eaten (Du et al., 2014). Extracts from various parts of *S. brachypetala*were active against bacteria that cause gastrointestinal infections; this

would explain the use of this plant in the traditional treatment of diarrhoea (Paiva et al., 2010). Furthermore, these extracts showed anti-oxidant, anti-bacterial and anti-malarial activities (Du et al., 2014), and were active against Alzheimer's disease, which was correlated to their anti-oxidant and probably anti-inflammatory properties (Hassaan et al., 2014).

The current work aimed to characterize the phenolic secondary metabolitesof*S. brachypetala*leaves using LC/HRESI/MS/MS and NMR. To evaluate its antioxidant activity *in vivo*, the nematode *Caenorhabditiselegans* was used, since it is a well-established model suitable to study stress resistance, aging, and longevity.

Materials and methods

Plant material

During the spring season (April-May 2012) *S. brachypetala* leaves were collected from trees grown in Orman Botanical Garden, Dokki, Giza, (Arab Republic of Egypt). The authenticity of the species was confirmed by Professor Dr. Mohamed El Gebaly (Professor of Taxonomy at the National Research Center, Egypt). The identity was further confirmed by DNA barcoding which was carried in our laboratory using *rbc*L as a marker gene. A voucher specimen was deposited at the herbarium of department of pharmacognosy, Faculty of Pharmacy, Ain Shams University, Egypt. Leaves sample was kept under accession number P8563 at IPMB drug store. The plant was collected during the spring season (April-May 2012).Specific permission was not required for research purpose because the plant

126 was grown as an ornamental tree in the Botanical Garden. The authors confirm
127 that the field studies did not involve endangered or protected species

128 **Plant material, extraction and isolation**

129 *S. brachypetala*leaves (1 kg) were exhaustively extracted with distilled
130 water (5 L). At low temperature, the extract was dried under vacuum followed by
131 alcohol extraction. Similarly, the soluble alcohol extract was dried under vacuum.
132 SBE dried powder of the aqueous alcohol (43g) was fractionated by column
133 chromatography using polyamide S6 column. Gradient elution was carried out to
134 obtain four main fractions. Fraction II showed only one major spot and was
135 compared to reference gallic acid, Fraction III was applied on top of Sephadex-
136 LH_{50} column for further purification; Fraction IV was purified using PPC
137 (preparative paper chromatography). Both Fraction III and IV were subjected to
138 further analysis by LC/ESI/MS^n. Compounds isolated from fraction III were
139 analyzed using ^{1}H-NMR spectroscopy.

140

141 **Solvents and chemicals**

142 HPLC analysis was performed using HPLC grade solvents. All other
143 chemicals used in the current work in the isolation of the compounds and in the
144 biological assays were purchased from Sigma-Aldrich Chemicals with analytical
145 grade.

146

147

148 **LC–HRESI-MS–MS**

149 The chromatographic analysis was performed on an HPLC Agilent 1200
150 series instrument, the column was Gemini 3 µm C18 110A° from Phenomenex
151 with dimensions 100 x 1 mm i.d. , protected with RP C18 100 A° guard column
152 with dimensions (5 mm x 300 µm i.d., 5 µm). The mobile phase was consisted of
153 two solvents (A) 2% acetic acid and (B) 90% MeOH, 2% acetic acid at a flow rate
154 of 50µL/min. The sample was dissolved in 5% MeOH and 2% acetic acid while
155 the sample injection volume was 10µl. A Fourier transform ion cyclotron
156 resonance mass analyzer was used equipped with an electrospray ionization (ESI)
157 system. X-calibur® software was used to control the system. Detection was
158 performed in the negative ion mode applying acapillary voltage of 36 V and a
159 temperature of 275 °C. The API source voltage was adjusted to 5 kV, and the
160 desolvation temperature to 275 °C. Nitrogen was used as a nebulizing gas with a
161 flow adjusted to 15 L/min. The analytical run time was 89 min and the full mass
162 scan covered the mass range from 150 to 2000*m/z* with resolution up to 100000
163 (Shaw, Werstuck&Chen, 2014).

164 **NMR**

165 For ^{1}H-NMR experiments, samples were dissolved in deuterated DMSO-
166 $d_6$and measured in 5mm tubes at 25 °C on a BRUKER 400 MHz NMR
167 spectrometer.

168

169

170 **HPLC Standardization of SBE**

The hydro-alcoholic extract (SBE) was standardized using an Agilent 1200 series HPLC instrument equipped with an Agilent quaternary pump connected to a photodiode array detector (PDA) with variable wavelengths. The separation was performed on a RP-C_{18} column with the following dimensions: 150 mm, 4.6mm, 5µm. The standard used was gallic acid (Sigma-Aldrich Chemicals) prepared in a dilution of 1.296 mg/ml in HPLC grade methanol to give a stock solution from which serial dilutions were prepared (0.001, 0.002, 0.003 and 0.004 mg/ml). All samples were tested using 4% acetic acid/ water (solvent A) and methanol (solvent B) in gradient program. The gradient program was 0-4 min 100% A, 4.01-10 min 50% A in 50% B , 10-20 min 20% A in 80 % B, 20-22 min 50% A in 50% B, 22-26 min 100% B, with flow rate 0.6 ml/min. 20 µl was injected onto the chromatograph, the detection was carried out at 280nmwavelength (Mradu et al., 2012). Different concentrations of the reference standard were plotted against the peak area to establish the calibration curve.

Antioxidant activity *in vitro*

DPPH$^{\bullet}$assay

The radical scavenging activity of SBE was assessed using the stable free radical DPPH$^{\bullet}$ (2,2-diphenyl-1-picrylhydrazyl). The assay was performed according to the standard technique described by Blois (1958) with some modifications to a 96-well microplate. In brief, 100 µl of DPPH solution (200 µM) were added to 100 µl of the SPE with concentrations ranges between (50-

1.25 µg/ml). In the dark at room temperature, the samples were incubated for 30 min. The absorbance was measured at 517nm. The ability of the samples to scavenge the DPPH radicals was calculated according to the following equation:

$$\text{DPPH scavenging effect (\%)} = [(A0 - A1)/A0] \times 100$$

Where A0 represents the control absorbance, and A1 the absorbance of SBE. All measurements were performed in triplicate. The EC_{50} value (µg SBE/ml) was estimated by sigmoid non-linear regression using adequate software.

TEAC persulfate decolorizing kinetic assay

Trolox equivalent antioxidant capacity (TEAC) assay uses green-coloured cation radicals of ABTS [2,2′-azinobis-(3-ethylbenzothiazoline-6-sulfonic acid)]. The assay was carried out to assess the quenching ability of the compounds in relation to the reactivity of Trolox, a water-soluble vitamin E analogue. TEAC assay was performed as described by (Re et al., 1999) adapted to a 96-well microplate. Initially, the reaction between 7 mM $ABTS^{\bullet+}$ and 2.45 mM potassium persulfate in water (final concentration) was used to generate $ABTS^{\bullet+}$ radical. The reaction was kept for 12-16 h (stock solution) in the dark and at room temperature. The $ABTS^{\bullet+}$ working solution was prepared in water. The absorbance of the working solution was (A_{734}= 0.7 ± 0.02). Trolox stock solution (11.5 mM) was prepared in ethanol and then diluted in water to give the working solution. 50 µl of Trolox or SBE were added in each individual well. Consequently, 250 µl of $ABTS^{\bullet+}$ working solution was added. The samples were kept for 6 min at room temperature, and then the absorbance was measured at 734 nm using a

spectrophotometer plate reader. All measures were performed in triplicate and repeated at least three times. The results were expressed in Trolox equivalent/mg of sample.

FRAP assay

FRAP assay, Ferric Reducing Antioxidant Power, was performed as previously reported by (Benzie& Strain, 1996) adapted to a 96-well microplate. The assay depends on the ability of the extract to reduce the ferric complex (2,4,6-tripyridyl-*s*-triazine – Fe^{3+}-TPTZ) to its ferrous form (Fe^{2+}-TPTZ) at low pH. 300 mM acetate buffer at pH 3.6, 10 mM TPTZ (2,4,6-tripyridyl-*s*-triazine) in 40 mMHCl and 20 mM $FeCl_3.6\ H_2O$ were used to prepare the FRAP working solution by mixing them in the ratio 10:1:1 prior to analysis. The fresh FRAP working solution was warmed to 37° C for 30 min prior to the assay. $FeSO_4.7H_2O$ was used as standard.

A freshly prepared FRAP working solution (175 µl) was added to the samples (25 µl), the reaction was kept for 7 min at 37° C. All measurements performed in triplicate and repeated three times. As a colorimetric assay, the reduction is indicated by development of an intense blue colour measured at 595 nm using a spectrophotometer microplate reader. FRAP values were showed as molFe(II)/mg of SBE sample.

Antioxidant activity *in vivo*

Caenorhabditiselegans strains and maintenance

Nematodes were maintained under standard conditions(on nematode growth medium – NGM - inoculated with living *E. coli* OP50, and incubated at 20°C),]. Age synchronized cultures were obtained by sodium hypochlorite treatment of gravid adults; the eggs were allowed to hatch in M9 buffer and larvae obtained were subsequently transferred to S-medium inoculated with living *E. coli* OP50 ($D.O_{600}$ = 1.0) (Stiernagle, 2006). In the current work the following *C. elegans* strains were used: Wild type (N2), TJ375 [*hsp-16.2::GFP(gpls1)*] and TJ356. All of them provided by the *Caenorhabditis*Genetic Center (CGC).

Survival assay under juglone induced oxidative stress

Synchronized worms (L1 larvae stage, N2 strain grown at 20°C in S-media inoculated with living *E. coli* OP50 – $D.O_{600}$= 1.0) were treated with 50 µg, 100 µg and 150 µg SBE/ml for 48 h, except the control group.. Then, juglone 80 µM was added as a single dose to the medium. 24 h after of the juglone treatment, the survivors were counted (Abbas and Wink, 2014). The result is presented as percentage of live worms, compared by one-way ANOVA followed by Bonferroni (post-hoc) correction.

Intracellular ROS in *C. elegans*

Synchronized worms (L1 larvae stage, N2 strain grown at 20°C in S-media inoculated with living *E. coli* OP50 – $D.O_{600}$= 1.0) were treated with 50 µg, 100 µg and 150 µg SBE/ml for 48 h, except the control group. After treatment, the worms were carefully washed in M9 buffer and then transferred to 1 ml of

CM-H_2DCF-DA 20 µM and incubated for 30 min at 20°C. To remove the excess of dye, the worms were washed once more with M9 buffer and finally analysed by fluorescence microscopy (λ_{Ex} 480/20 nm; λ_{Em} 510/38 nm). The worms were paralyzed with sodium azide 10 mM and placed on a glass slide. Images were taken from at least 30 worms at constant exposure time. The relative fluorescence of the whole body was determined densitometrically using Image J software. The results are shown as mean pixel intensity (mean ± SEM) and tcompared by one-way ANOVA followed by Bonferroni (post-hoc) correction.

Quantification of hsp-16.2::GFP expression

Synchronized transgenic *C. elegans*TJ375 [expressing *hsp-16.2::GFP(gpls1)*] were grown at 20°C in S media with living *E. coli* OP50 ($D.O_{600\ nm}$= 1.0). L4 worms were treated for 48 h with 50, 100 and 150 µg SBE/ml, except the control group. Then they were exposed to juglone 20 µM for 24 h and finally analysed by fluorescence microscopy (λ_{Ex} 480/20 nm; λ_{Em} 510/38 nm). The mutant strain contains *hsp-12.6* promoter coupled to the gene encoding GFP (green fluorescence protein), whose expression is directly quantified by observing the fluorescence intensity of the GFP reporter in the pharynx of the worm. The worms were paralyzed with sodium azide 10 mM and placed on a glass slide. Images were taken from at least 30 nematodes using 20X objective lens at constant exposure time. The relative fluorescence of the pharynx was determined densitometrically using imageJ software. The results are shown as mean pixel intensity (mean ± SEM) and then compared by one-way ANOVA followed by Bonferroni (post-hoc) correction.

Subcellular DAF-16 localization

Synchronized transgenic TJ356 worms (L1 larvae grown in S media at 20°C with living *E. coli* OP50 - D.$O_{600\ nm}$= 1.0),which have a DAF-16::GFP fusion protein as reporter, were treated for 72 h with 50, 100 and 150 µg SBE/ml, except the control group. In M9 buffer, the worms were paralyzed with sodium azide 10 mM and placed on a glass slide. Images were taken from at least 30 worms using 10X objective lens at constant exposure time. According to DAF-16::GFP fusion protein major location, the worms were sorted in three categories: cytosolic, intermediate and nuclear. The results are shown as percentage (mean ± SEM) and compared by one-way ANOVA followed by Bonferroni (post-hoc) correction.

Results and discussion

Identification of the isolated flavonoid glycosides by NMR

Two flavonoid glycosides (myrecitin-3-*O*-*α*-L-$^{1}C_{4}$-rhamnoside) and (quercetin-3- *O*- *α*-L-$^{1}C_{4}$-rhamnoside), were isolated and identified from SBEfor the first time.

Compound **1** (2.3g) was isolated as yellow crystalline powder. On PC, it showed a dark purple spot under short UV light. $R_f$values: 24.5 (BAW) and 13.5 (6% AcOH). It gave a dirty green colour with $FeCl_3$ spray reagent which is specific for phenolics. Also, its UVspectrum showed two bands at λ_{max}MeOH (350nm band

I and 206nm band II), which are indicative the flavone nucleus. It showed a bathochromic shift (19nm) on addition of sodium methoxide and (66nm) in band II with sodium acetate to prove that the 3', 4', 5' and 7 OH positions are free. The ^{1}H-NMR spectra indicated the absence of the signal for H-3, the presence of aromatic proton signals at δ=6.15*ppm* (1H, *s*, H-8) and δ=6.31*ppm* (1H, *s*, H-6), presence of *O*-glycosidicanomeric signal at δ=5.2*ppm* (1H, *s*, H-1") and signal for methyl of rhamnose at δ=1.51*ppm* (3H, S, CH_3rhamnose). UV as well as ^{1}H-NMR chemical shifts were found to be similar to those previously reported for myrecitin-3-*O*-*α*-L-$^1C_4$-rhamnoside. Consequently, compound **1** was confirmed to be myrecitin-3-*O*-*α*-L-$^1C_4$-rhamnoside (Hayder et al., 2008).

Compound 2 (0.39g) was obtained as yellow crystalline powder. On PC, it showed a dark purple spot under short UV light. $R_f$values: 22.5 (BAW) and 7.5 (6% AcOH). It gave a dirty green colour with the $FeCl_3$spray reagent. Also, its UV spectrum showed two bands at λ_{max}MeOH (350nm band I and 206nm band II) which indicated the presence of a flavone nucleus. It showed a bathochromic shift (30nm) on addition of sodium methoxide and (20nm) in band II with sodium acetate indicating that the 3', 4" and 7 OH positions are free. From these data we conclude that compound **2**corresponds to quercetin-3-*O*-*α*-L-$^1C_4$-rhamnoside.

The ^{1}H-NMR spectrum of compound **2** indicated the absence of the signal for H-3, the presence of aromatic proton signals at δ =7.199 (1H, *d*, J=2.5 *Hz*, H-2'), δ=6.909 (1H, *dd*, J=2.5 *Hz*, 8 *Hz*, H-6'), δ =6.882 (1H, *d*, J=8 *Hz*, H-5'), presence of *O*-glycosidicanomeric signal at δ=5.214ppm (1H, *S*, H-1") and a signal for methyl of rhamnose at δ=1.242 *ppm* (3H, *s,* CH_3rhamnose).UV as well as ^{1}H-NMR

chemical shifts were found to be similar to those previously reported for quercetin-3-*O*-α-L-$^1C_4$-rhamnoside. Consequently, compound **2** was identified asquercetin-3-*O*-α-L-$^1C_4$-rhamnoside (Ma et al., 2005).

Identification of constituents by LC/HRESI/MS/MS

HPLC-MS plays an important role in the separation and identification of complex plant mixtures. Among its main advantages is the high sensitivity and specificity which can be used both for volatile and non-volatile compounds (Dumont & Beal, 2011).

A total of 43secondary metabolites were identified from SBE, its fractions and sub-fractions using LC/ESI/MS/MS (Table 1). LC/HRESI/MS/MS profiles of SBE, its fractions and sub-fractions are shown in Figures (1-5). Different classes of phenolics were discovered, which will be discussed in the following:

Flavonoid glycosides

The negative ion mode profile of LC-ESI-MS/MS showed a major peak (peak area 4.85%) with a $[M-H]^-$at *m/z* 477 representing quercetin-3-*O*-glucouronide **(8)** and a fragment at *m/z* 301 for the deprotonated quercetinaglycone. The difference of 176 mass units indicates a glucuronic acid moiety; the fragment at *m/z* 151 of ring A in quercetinaglycone moiety, confirming the quercetinaglycone identity (Saldanha, Vilegas&Dokkedal,2013). Another peak for the deprotonated ion *m/z* 447 was identified as quercetin-3- rhamnoside**(13)** according to literature data (Saldanha, Vilegas&Dokkedal,2013), accompanied with a fragmentation at *m/z* 301 due to cleavage of the *O*-glycosidic bond releasing free aglycone and loss of a sugar moiety.

Another molecular ion peak (*m/z* 431) was identified as kaempferol-3-*O*-rhamnoside **(15)** (Diantini, Subarnas&Lestari, 2012) with a major fragment at *m/z* 285 corresponding to the kaempferolaglycone (Diantini, Subarnas& Lestari, 2012).

Quercetin-3-*O*-hexoside isomers **(37)(38)** were identified by a molecular peak of *m/z* 463 accompanied by fragment ions at *m/z* 301 indicative for a quercetinaglycone.Flavonolaglycones like quercetin produce a characteristic ion the deprotonated fragment $[M–H]^-$, moreover, they produce ions corresponding to retro-Diels-Alder (RDA) fragmentation in thering C, involving 1,3-scission (Sannomiya,Montoro&Piacent, 2005). Kaempferol-3-*O*-rutinoside **(40)** as an example for flavonol-*O*-dihexosides was identified with *m/z* 593 (Valko et al., 2007), which was further confirmed in comparison with an authentic reference substance.

The pka values for each of the compounds confirmed the sequence of elution all over the peaks. Based on MS–MS fragmentation a $[M–H]^-$signal at *m/z* 519 was assigned to isorhamnetin acetyl-glucoside (an acylatedflavonol glycoside) **(36)** which is characterized by the loss of a glucose and a complete acetylglucose unit, producing fragments with strong intensity at *m/z* 357 [M-162-H] and at *m/z* 315 [M-162–42- H], respectively.

Galloylated flavonoid glycosides

A number of galloylated derivatives were identified as major peaks with $[M-H]^-$at *m/z* 631. According to literature data (Saldanha, Vilegas&Dokkedal,2013), they represent myrecitin-3-*O*-(2"-*O*-galloyl)-hexoside

and its isomer **(6) (7)**.Informative ions are: deprotonated molecular mass $[M-H]^-$ (*m/z* 631), fragment ion peak for deprotonated myrecitinhexoside (*m/z* 479), and a deprotonated myrecitin at *m/z* 317.Two peaks with the same pattern were detected suggesting the presence of sugar isomers.

Major peaks of quercetin-3-*O*-(2"-*O*-galloyl)-hexoside and its isomer **(9) (10)**, showed deprotonated molecule peak $[M-H]^-$ at *m/z* 615, a fragment ion peak for the deprotonated quercetinhexoside (*m/z* 463), and for the deprotonated quercetinaglycone at *m/z* 301(Saldanha, Vilegas&Dokkedal,2013).

Additionally, the molecular ion peak at *m/z* 599, which is indicative for the deprotonated quercetin hexose protocatechuic acid and its sugar isomer **(11)(12)**;fragment ions at *m/z* 463 and *m/z* 300 may be due to the loss of the hexose and the protocatechuic acid moiety, respectively (Abdel-Hameed, Bazaid& Salman, 2013). Furthermore, the molecular ion peak $[M-H]^-$at *m/z* 601 and its deprotonated fragment at *m/z* 449) were identified as myrecitin-3-*O*-(2"-galloyl)-pentoside (Saldanha, Vilegas&Dokkedal,2013), the difference of *m/z* 152 is due to a loss of pentose residue from the molecule. The presence of two molecular ion peaks with the same fragmentation pattern but different retention times indicates the presence of isomers. Similarly, the peak at *m/z* 585, with the difference in aglycone moiety (quercetin instead of myrecitin), represents the deprotonated molecular ion of quercetin-3-*O*-(2"-galloyl)-pentoside**(28)** (Saldanha, Vilegas&Dokkedal,2013) and deprotonated fragments at (*m/z* 433) and (*m/z* 301) suggest the sequential loss of a pentose and galloyl moiety.

393 **Hydroxybenzoic acid derivatives**

394 This class was represented by a deprotonated molecular ion peak at *m/z*
395 343indicative for galloylquinic / epiquinic acid **(32)(33)** and the deprotonated
396 fragments at *m/z* 191, and *m/z* 85; fragment *m/z* 191beingconsistent with quinic
397 acid (Clifford, Stoupi&Kuhnert, 2007). The presence of two peaks with *m/z*
398 343butdifferent retention times can beexplained by the presence of quinic acid
399 and its isomer epiquinic acid **(27)(28)** (Eliel&Ramirez, 1997).

400 **Isoflavones**

401 A minor peak of daidzeinaglycone**(1)** was recognized as a deprotonated
402 peak at *m/z* 253.

403 **Dihydrochalcones**

404 A hexoside derivative ofphloretin, a characteristic and quite common aglycone
405 previously reported in apple, was identified in SBE as phloretin-3-*O*-
406 xyloglucoside **(42)**with *m/z* 567 and a major ion peak at *m/z* 273 corresponding to
407 the aglycone of phoretin (Balazs et al, 2012).

408 **Procyanidins**

409 A procyanidin dimer-hexoside **(43)** was identified and recognized at *m/z* 737
410 with fragmentation pattern as follows: A product ion of *m/z*611 containing the
411 galactoside was formed by the loss of gallic acid (126 Da). However, the second
412 product ion with*m/z* 449 was detected in the spectrum indicates the loss of both the
413 gallic acid and the sugar moiety (Sies and Stahl, 1995). A procyanidintrimer**(24)** was

identified according to its deprotonated base peak at *m/z* 850andits deprotonated fragments at *m/z* 697, 425 and 407, which are produced by a cleavage of the interflavan bond through a quinine-methide (QM) cleavage (Passos, Cardoso&Domingues,2007) to give (*m/z* 425) then a loss of water molecule to yield *m/z* 407 in agreement with a procyanidintrimer MS fragmentation pathway (Passos, Cardoso&Domingues,2007).

Hydrolysable tannins

For trigalloyl hexose isomer **(20)** a $[M-H]^-$was identified with *m/z* 635. The contribution of the major peak (*m/z* 483) is due to the presence of a digalloyl-hexose moiety. Besides, two intermediate ions were detected at *m/z* 271 and *m/z* 211. They are indicative formono and di-galloyl-hexose; the elimination of a hexose moiety from monogalloyl-hexose was detected which subsequently lead to the formation of the deprotonated gallic acid at *m/z* 169 (Poay, Kiong& Hock,2011).

Represented by a deprotonated parent ion peak at *m/z* 495 for digalloylquinic acid **(2) (4)**, different positional isomers arise from the difference in hydroxyl attachment site giving rise to peaks of same *m/z* value. The identification was done according to the identity of the obtained peaks as follows: a $[M–H]^-$ at *m/z* 343 indicates the loss of a galloylmoiety from the parent peak and fragmentation showed fragments at *m/z* 191 and *m/z* 169, corresponding to quinic acid andgallic acid moieties, respectively (Sannomiya,Montoro&Piacent, 2005). Compound **(5)** with *m/z* 483, identified as digalloyl hexose, showed an ion peak typical for the dimer analogue of *m/z* 169 produced by gallic acid.

437 **Methyl and acetyl flavonoid glycosides**

438 A peak at *m/z* 963 is typical for deprotonated
439 methoxylatedcastalagin/vescalagin**(25)** showing a major peak at m/*z* 933,
440 corresponding to the polyphenol castalagin or its isomer vescalagin (Rauha,
441 Wolfender&Salminen, 2001).

442 Two acetyl flavonoid glycosides were detected luteolin-7-*O*-hexosyl-8-*C*-
443 (6"-acetyl)-hexoside (**35)** with *m/z* 651. The detected fragments at *m/z* 179, 151
444 provide the evidence thatluteolin was the aglycone of compound **(35)** (Simirgiotis
445 et al., 2013). Compound (**41)** with a [M−H]− ion at *m/z* 687 showed fragments at
446 *m/z* 651, 489, 327. These ions match with the MS data previously reported for
447 compound (**41)[**luteolin-5-*O*-hexosyl-8-*C*-(6"-acetyl)-hexoside derivative], full MS
448 at (*m/z* 651) after the loss of 38 amu and thus was tentatively assigned to its
449 analogue luteolin-7-*O*-hexosyl-8-*C*-(6"-acetyl)-hexoside **(35)** (Masika,
450 Sultana&Afolayan,2004).

451

452 **Methylflavone, flavanol and flavonol**

453 A methyl-flavone was identified as tricin-7-*O*-neohesperidoside **(44)** from
454 its exact mass (*m/z* 638) $[M-H]^-$; by taking into consideration the additional mass of
455 30 for the extra methoxy group on the $[M-H]^-$ ion. The major fragments of **(38)**
456 were at *m/z* 492 and 330 corresponding, respectively, to ions $[M-H-146]^-$ and [M-
457 H-146-162]. The losses of 146 and 162 Da are characteristic for rhamnose and

glucose moieties, respectively, and the ion at *m/z* 330 is characteristic of the aglyconetricin (Paiva et al., 2010).

A flavanol was represented by a deprotonated parent peak for (epi) catechingallateat*m/z* 441**(31)** and its deprotonated fragments at *m/z* 289, 169 and 135 (MarkowiczBastos et al., 2007). The fragment at *m/z* 289 for the deprotonated (epi) catechin (Ivanova et al., 2011), *m/z* 169 for the galloyl moiety, and *m/z* 135 for ring (A) of flavones nucleus. As an example of the flavonolisorhamnetin**(30)**, a deprotonated molecular ion peak was detected at *m/z* 315 with deprotonated fragments at (*m/z* 301, *m/z* 151) (Snache- Rabaneda et al., 2003).

Standardization of SBE using HPLC

The SBE showed an intense peak at R_t 3.983 min corresponding to gallic acid (identified by peak matching with a gallic acid standard). Through the standardization experiment, it was shown that each mg SBE constitutes 0.0022 mg gallic acid. The calibration curve showed good linearity for gallic acid (reference compound) in the range of 0.3 up to 1 mg/ml with correlation coefficient (R2) 0.999.

Antioxidant activities *in vitro* and *in vivo*:

Antioxidant activity *in vitro*

Total phenolic contents of SBE were 376 mg of caffeic acid equivalents (CAE)/g SBE while the total flavonoid content was 67.87 mg (quercetin equivalents)/g SBE. The antioxidant activity of SBE was evaluated *in vitro* using

three different assays, DPPH, ABTS and FRAP. These methods are widely employed for the antioxidant activity evaluation of pure compounds, plant extracts, as well as food items because long-lived radicals such as $DPPH^{\bullet}$ and $ABTS^{\bullet+}$ as well as $FeSO_4$are sensitive and reliable (Prior, Wu&Schaich, 2005). All methods revealed a strong antioxidant capacity of SBE (Table 2).

Antioxidant activity *in vivo* in *C. elegans*

Survival Assay

Juglone *(*5-hydroxy-1,4-naphthoquinone) is a natural quinine from *Juglansregia* with toxic pro-oxidant activity (Saling et al., 2011) . Exposure of *C. elegans* to a high concentration of juglone kills the worms; however, antioxidant compounds can prevent such an effect. According to our results (Figure 6), worms pre-treated with SBE showed an increased survival rate (up to 41 %), when compared with the control group (11%), which was treated with juglone alone. The increased survival rate indicates that SBE works efficiently as an antioxidant *in vivo*. Similar results have been obtained with other antioxidant polyphenols, such as EGCG from green tea, anthocyanins from purple wheat and aspalathin from Rooibos tea (Abbas& Wink. 2014; Chen et al., 2013).

Influence of SBE on intracellular ROS in *C. elegans*

To assess the intracellular concentration of ROS (reactive oxygen species) and to evaluate a potential antioxidant activity *in vivo*, the membrane permeable reagent

2',7'- dichlorofluorescindiacetate (CMH_2DCF-DA) was used. The reagent becomes deacetylated to a non-fluorescent compound by intracellular esterases. The deacetylated form is oxidized in the presence of ROS, especially H_2O_2, forming high fluorescent compound 2', 7'- dichlorofluorescein (DCF) which can to be analysed by fluorescence microscopy. In our experiments, worms were treated for 48 h with three different concentrations of SBE (50, 100 and 150 µg/ml) and then analysed by fluorescence microscopy. The images reveal that the SBE treated worms exhibited significantly lower fluorescence intensity in comparison to the untreated control group (Figure 7). The decrease in the fluorescence, measured through pixel intensity, was dose-dependent and reachs up to 72%for the highest tested concentration, indicating that SBE is capable to effectively scavenge the ROS *in vivo*.

Quantification of *hsp-16.2*::GFP expression via fluorescence microscopy

Heat shock proteins (HSPs) are virtually found in all living organisms. Increase in HSP levels correlates with exposure to environmental stress conditions that can induce protein damage such as high temperature and presence of oxidants. HSP play an important role for aging and longevity (Swindell, 2009).

To assess the ability of SBE to suppress *hsp-16.2*::GFP expression, worms from the mutant strain TJ375 were used. *hsp*-16.2::GFP expression was induced by juglone treatment. Results revealed that those worms pre-treated with SBE had a significantly lower expression of *hsp*-16.2::GFP, monitored by fluorescence microscopy. The reduction of *hsp*-16.2::GFP expression was dose-dependent and

522 up to 60% in the 150 µg SBE/ml group, in comparison with the control group
523 (Figure 8). These findings correlate with the demonstrated ability of SBE in
524 increasing the mean survival rate in response to acute oxidative stress (caused by
525 juglone; Figure 6) and suppress ROS formation *in vivo* (Figure 8). Similar results
526 have been reported for other phenolic antioxidants, such as EGCG (Abbas and
527 Wink, 2014).

528 **Subcellular localization of DAF-16**

529

530 DAF-16, a forkhead transcription factor (FOXO) family member, in its
531 phosphorylated form, it remains arrested in the cytosol (inactive form).The
532 dephosphorylated active form migrates into the nucleus and triggers the activity of
533 several target genes related to oxidative stress response and lifespan regulation in
534 both, *C. elegans* and mammals (Mukhopadhyay&Tissenbaum, 2006).

535 In another set of experiments, we investigated whether the antioxidant
536 effects observed, were related to DAF-16/FOXO translocation into the nucleus.
537 Worms (transgenic strain TJ356) were treated with SBE and submitted later to
538 fluorescence microscopy. As illustrated in Figure 9, a high percentage of the treated
539 worms showed nuclear localization pattern of DAF-16/FOXO (up to 78%), while
540 in the untreated control group, only 5% of the worms exhibited a nuclear
541 localisation pattern. This finding strongly suggests that the ability of SBE to
542 enhance oxidative stress resistance in *C. elegans* is DAF-16/FOXO dependent,
543 similar to the situation with other phenolic antioxidants (Abbas and Wink. 2014;
544 Chen et al. 2013).

Conclusions

The current study resulted inthe identification of different phenolic metabolite classes including flavonoid glycosides, procyanidins, anthocyanins, dihydrochalcones, and hydroxybenzoic acid derivatives. Myricetin-3-*O*-*α*-L-$^{1}C_{4}$-rhamnoside, quercetin-3-*O*--L-$^{1}C_{4}$-rhamnoside, and gallic acid were reported for the first time from the leaves of *S. brachypetala*.

SBE is rich in phenolics, especially flavonoid glycosides such as quercetin which are known as powerful antioxidants *in vitro* (Bouktaib, Atmani&Rolando, 2002). Potential health effects of polyphenols have been discussed: Several studies reported the ability of quercetin to ameliorate pathological conditions linked to ROS such as oxidation of LDL-cholesterol, to counteract cardiovascular risks (Chopra et al. 2000), to protect primary neurons against to Aβ deposits (Ansari et al. 2009). Furthermore, antioxidants are beneficial for chronic inflammation (Comalada et al. 2005; Shoskes et al. 1999) and can avoid Ca^{2+}-dependent cell death (Sakanashi et al., 2008)

Our study showed that SBE exhibits a strong antioxidant activity *in vitro* as well as *in vivo*. It is able to decrease ROS production and attenuates *hsp16.2* expression under oxidative stress conditions in *C. elegans*. We assume that a modulation of the DAF-16/FOXO transcription factor by the phenolics is responsible for the observed antioxidant effects. The leaf extract can increase the nuclear location of DAF-16, thereby activating many important biological processes including target genes related to stress resistance and longevity.

Further *in vivo* experiments are needed to develop the polyphenols of *S. brachypetala* into a useful nutraceuticals or phytomedicine.

Conflict of Interest: There is no conflict of interest.

References

Abbas, S. and Wink, M., 2014. Green Tea Extract Induces the Resistance of Caenorhabditis elegans against Oxidative Stress. Antioxidants 3, 129-143.

Abdel-Hameed, S.S., Bazaid, S.A., Salman, M.S., 2013. Characterization of the phytochemical constituents of Taif rose and its antioxidant and anticancer activities. Biomed Research International 2013, 345-465.

Angerhofer, C.K., Maes, D., Giacomoni, P., 2008. The use of natural compounds and botanicals in the development of anti-aging skin care products. Skin Aging Handbook: an integrated Approach to Biochemistry and Product Development. New York: William Andrew Inc, 205-63.

Ansari, M.A., Abdul, H., Joshi, G., Opii, W., Butterfield, D.A., 2009. Protective effect of quercetin in primary neurons against Aβ (1–42): relevance to Alzheimer's disease. The Journal of nutritional biochemistry 20, 269-275.

Balazs, A., Tóth, M., Blazics, B., Héthelyi, E., Szarka, S., 2012. Investigation of dietary important components in selected red fleshed apples by GC-MS and LC-MS. Fitoterapia 83, 1356-63.

Barja, G., 2004. Free radicals and aging. Trends in neurosciences 27, 595-600.

588 Bastos, L.A.S., Catharino, R., Alexandra, C., Sawaya, H., Carvalho, P., Eberlin, M., 2007.
589 Phenolic Antioxidants Identified by ESI-MS from Yerba Maté (Ilex paraguariensis)
590 and Green Tea (Camelia sinensis) Extracts. Molecules 12, 423-432.
591 Benzie, I.F. and Strain, J., 1996 The ferric reducing ability of plasma (FRAP) as a
592 measure of "antioxidant power": the FRAP assay. Analytical biochemistry 239, 70-
593 76.
594 Blois, M.S., 1958. Antioxidant determinations by the use of a stable free radical.
595 Brenan, J.,1967. Leguminosae Part 2, Caesalpinioideae. Flora of tropical East Africa.
596 Crown Agents, London.
597 Bouktaib, M., Atmani, A., Rolando, C., 2002. Regio-and stereoselective synthesis
598 of the major metabolite of quercetin, quercetin-3-< i> O</i>-β-d-glucuronide.
599 Tetrahedron Letters 43, 6263-6266.
600 Chen, W., Müller, D., Richling, E., Wink, M., 2013. Anthocyanin-rich purple wheat
601 prolongs the life span of Caenorhabditis elegans probably by activating the DAF-
602 16/FOXO transcription factor. Journal of agricultural and food chemistry 61, 047-
603 3053.
604 Chopra, M., Fitzsimons, P., Strain, J., Thurnham, D., Howard, A., 2000. Nonalcoholic red
605 wine extract and quercetin inhibit LDL oxidation without affecting plasma
606 antioxidant vitamin and carotenoid concentrations. Clinical Chemistry46, 1162-
607 1170.
608 Clifford, M.N., Stoupi, S., and Kuhnert, N., 2007. Profiling and characterization by LC-
609 MSn of the galloylquinic acids of green gea, tara tannin, and tannic acid. Journal of
610 agricultural and food chemistry 55, 2797-2807.

611 Comalada, M., Camuesco, D., Sierra, S., Ballester, I., Xaus, J., Glvez, J., Zarzuelo, A.,
612 2005. In vivo quercitrin anti-inflammatory effect involves release of quercetin,
613 which inhibits inflammation through down-regulation of the NF-κB pathway.
614 European journal of Immunology 35, 584-592.
615 Debnath, T., Kim, D. and Lim, B.,2013. Natural products as a source of anti-inflammatory
616 agents associated with inflammatory bowel disease. Molecules 18, 7253-7270.
617
618 Diantini, A., Subarnas, A., Lestari, K., 2012. Kaempferol-3-O-rhamnoside isolated from
619 the leaves of Schima wallichii Korth. inhibits MCF-7 breast cancer cell
620 proliferation through activation of the caspase cascade pathway. Oncol Lett, 3,
621 1069-1072.
622 Drewes, S.E. and Fletcher, I.P.,1974. Polyhydroxystilbenes from the heartwood of Schotia
623 brachypetala. Journal of the Chemical Society, Perkin Transactions 1, 961-962.
624 Du, K., Marston, A., van Vuuren, S., van Zyl, R., Coleman,C., Zietsman, P., Bonnet, S.,
625 Ferreira, D., van der Westhuizen, J., 2014. Flavonolacyl glucosides from the aril of
626 Schotia brachypetala Sond. and their antioxidant, antibacterial and antimalarial
627 activities. Phytochemistry Letters, 124-129.
628 Dumont, M. and Beal, M.F., 2011. Neuroprotective strategies involving ROS in Alzheimer
629 disease. Free radical biology and medicine 51, 1014-1026.
630 Eliel, E.L. and Ramirez, M.B., 1997. (−)-Quinic acid: configurational (stereochemical)
631 descriptors. Tetrahedron: Asymmetry 8, 3551-3554.

632 Efferth, T. and Wink, M., 2010. Chemical-biology of natural products from medicinal
633 plants for cancer therapy, in Alternative and Complementary Therapies for Cancer,
634 M. Alaoui-Jamali, Editor. Springer US. p. 557-582.
635 Fujiki, H., Suganuma, M., Okabe, S., Sueoka, E., Suga, K., Imai, K., Nakachi, K., Kimura,
636 S., 1999. Mechanistic findings of green tea as cancer preventive for humans.
637 Experimental Biology and Medicine 220, 225-228.
638 Hanganu, D., Vlase, L. and Olah, N., 2010. LC/MS analysis of isoflavones from Fabaceae
639 species extracts. Farmacia 2, 177-183.
640 Hassaan, Y., Handoussa, H., El-Khatib, A., Linscheid, M., El-Sayed, N., Ayoub, N., 2014.
641 Evaluation of plant phenolic metabolites as a source of alzheimer's drug leads.
642 BioMed Research International, 10.
643 Hayder, N., Hayder, N., Skandrani, I., Kadri, M., Steiman, R.,Mariotte, A.,Ghedira,
644 K., Dijoux-Franca, M., Chekir-Ghedira, L., 2008. In vitro antioxidant and
645 antigenotoxic potentials of myricetin-3-o-galactoside and myricetin-3-o-
646 rhamnoside from Myrtus communis: modulation of expression of genes involved in
647 cell defence system using cDNA microarray. Toxicology In Vitro 22, 567-81.
648 Poay, T., Kiong, L., Hock, C., 2011. Characterisation of galloylated cyanogenic
649 glucosides and hydrolysable tannins from leaves of Phyllagathis rotundifolia by
650 LC-ESI-MS/MS. Phytochemical Analysis 22,516-25.
651 Ivanova, V., Dörnyei, A., Márk, L., Vojnoski, B., Stafilov, T., Stefova, M., Kilár,
652 F., 2011. Polyphenolic content of Vranec wines produced by different vinification
653 conditions. Food Chemistry 124, 316-325.

654 Kim, H.P., Son, K., Chang, H., Kang, S., 2004. Anti-inflammatory plant flavonoids
655 and cellular action mechanisms. Journal of pharmacological sciences 96, 229-245.
656 Ma, X., Tian,W., Wu,L., Cao, X., Ito, Y., 2005. Isolation of quercetin-3-O-l-
657 rhamnoside from Acer truncatum Bunge by high-speed counter-current
658 chromatography. Journal of Chromatography A 1070, 211-214.
659 Masika, P.J., Sultana, N. and Afolayan, A.J., 2004. Antibacterial Activity of Two
660 Flavonoids Isolated fromSchotia latifolia. Pharmaceutical Biology. 42, 105-108.
661 McGaw, L., Jäger, A., and Van Staden, J., 2002. Isolation of antibacterial fatty
662 acids from *Schotia brachypetala*. Fitoterapia 73, 431-433.
663 Mradu, G.,Saumyakanti, S., Sohini, M., Arup, M., 2012. HPLC profiles of
664 standard phenolic compounds present in medicinal plants. International Journal of
665 Pharmacognosy and Phytochemical Research 4, 162-167.
666 Mukhopadhyay, A., Oh, S.W., Tissenbaum, H. A., 2006. Worming pathways to and
667 from DAF-16/FOXO. Experimental gerontology 41, 928-934.
668 Paiva, P.M.G., Gomes, F.S., Napoleão, T.H., Sá, R.A.,Correia, M.T.S., Coelho.,
669 L.C., 2010. Antimicrobial activity of secondary metabolites and lectins from plants.
670 Current Research, Technology and Education Topics in Applied Microbiology and
671 Microbial Biotechnology.
672 Passos, C.P., Cardoso, S.M., Domingues, M.R., 2007. Evidence for galloylated
673 type-A procyanidins in grape seeds. Food Chemistry 105,1457-1467.
674 Patel, K., Brown, V.,, Jones, D., Britton, R., Hemingway, D., Miller, A., West,
675 KP, Booth, TD, Perloff, M, Crowell, JA, Brenner, DE, Steward, WP, Gescher,

AJ, Brown, K., 2010. Clinical pharmacology of resveratrol and its metabolites in colorectal cancer patients. Cancer research 70, 7392-7399.

Pendergrass, W.R., Penn, P., Possin, D., Wolf, N., 2006. Cellular debris and ROS in age-related cortical cataract are caused by inappropriate involution of the surface epithelial cells into the lens cortex. Molecular Vision 12, 712-24.

Prior, R.L., Wu, X. Schaich, ,K., 2005. Standardized methods for the determination of antioxidant capacity and phenolics in foods and dietary supplements. Journal of agriculture and Food Chemistry 53, 4290−4302.

Re, R., Rea, R., Pellegrinia,N., Proteggentea,A., Pannalaa, A., Yanga, M., Catherine, E., 1999 Rice-, Antioxidant activity applying an improved ABTS radical cation decolorization assay. Free radical biology and medicine 26, 1231-1237.

Rauha, J.P., Wolfender, J.L., Salminen, J.P., 2001. Characterization of the polyphenolic composition of purple loosestrife (Lythrum salicaria). Zeitschrift fur Naturforschung C 56, 13-20.

Rossi, L., Mazzitelli, S., Arciello, M., Capo, C.R., Rotilio, G., 2008. Benefits from dietary polyphenols for brain aging and Alzheimer's disease. Neurochemical research 33, 2390-2400.

Saldanha, L.L., Vilegas,W., Dokkedal, A., 2013. Characterization of flavonoids and phenolic acids in Myrcia bella Cambess. using FIA-ESI-IT-MS(n) and HPLC-PAD-ESI-IT-MS combined with NMR. Molecules 18, 8402-16.

Saling, S.C., Comar, J., Mito, M., Peralta, R., Bracht, A., 2011. Actions of juglone on energy metabolism in the rat liver. Toxicology and Applied Pharmacology 257, 319-327.

699 Sakanashi, Y., Oyama, K., Matsui, H., Oyama, T., Oyama, T., Nishimura, Y.,
700 Sakai, H., Nishimura, Y., 2008. Possible use of quercetin, an antioxidant, for
701 protection of cells suffering from overload of intracellular Ca2+: A model
702 experiment. Life Sciences 83, 164-169.
703 Sanchez-Rabaneda, F., Jáuregui, O., Casals, I., Andrés-Lacueva, C., Izquierdo-
704 Pulido, M., Lamuela-Raventós, R., 2003. Liquid chromatographic/electrospray
705 ionization tandem mass spectrometric study of the phenolic composition of cocoa
706 (*Theobroma cacao*). Journal of Mass Spectrometry 38, 35-42.
707 Sannomiya, M., Montoro, P., Piacent, S., 2005. Application of liquid
708 chromatography/electrospray ionization tandem mass spectrometry to the analysis
709 of polyphenolic compounds from an infusion of *Byrsonima crassa* Niedenzu. Rapid
710 Commun Mass Spectrom 19, 2244-50.
711 Shaw, P.X., Werstuck, G. and Chen, Y. 2014. Oxidative stress and aging diseases.
712 Oxidative medicine and cellular longevity.
713 Shoskes, D.A., Zeitlin, S.I., Shahed, A., Rajfer,J., 1999., Quercetin in men with
714 category III chronic prostatitis: a preliminary prospective, double-blind, placebo-
715 controlled trial. Urology 54, 960-963.
716 Sies, H. and Stahl, W., 1995. Vitamins E and C, beta-carotene, and other
717 carotenoids as antioxidants. The American journal of clinical nutrition 62 1315S-
718 1321S.
719 Simirgiotis, M.J., Schmeda-Hirschmann, G., Bórquez, J., Kennelly, E., 2013. The
720 Passiflora tripartita (Banana Passion) fruit: a source of bioactive flavonoid C-

721 glycosides isolated by HSCCC and characterized by HPLC-DAD-ESI/MS/MS.
722 Molecules 18, 1672-92.
723 Stiernagle, T., 2006. Maintenance of C. elegans, WormBook, ed. The C. elegans
724 Research Community. WormBook. http://www. wormbook. org.
725 Swindell, W.R., 2009. Heat shock proteins in long-lived worms and mice with
726 insulin/insulin-like signaling mutations. Aging 1, 573.
727 Valko, M., Leibfritz, D., Moncol, J., Cronin, M.T., Mazur, M., Telser, J., 2007.
728 Free radicals and antioxidants in normal physiological functions and human
729 disease. The international journal of biochemistry & cell biology 39, 44-84.
730 Valko, M., Izakovic,M., Mazur, M., Rhodes, C. and Telser, J., 2004. Role of
731 oxygen radicals in DNA damage and cancer incidence. Molecular and cellular
732 biochemistry 266, 37-56.
733 Van Wyk, B.E. and Wink, M., 2004. Medicinal plants of the world: an illustrated
734 scientific guide to important medicinal plants and their uses. Timber Press (OR).
735 Watt, J.M. and Breyer-Brandwijk, M., 1932. The medicinal and poisonous plants of
736 Southern Africa. The medicinal and poisonous plants of southern Africa.
737 Widlansky, M.E., Hamburg, N., Anter, E., Holbrook, M., Kahn, D., Elliott, J.,
738 Keaney, J., Vita, J., 2007. Acute EGCG supplementation reverses endothelial
739 dysfunction in patients with coronary artery disease. Journal of the American
740 College of Nutrition 26, 95-102.
741 Wolfram, S., 2007. Effects of green tea and EGCG on cardiovascular and metabolic
742 health. Journal of the American College of Nutrition 26, 373S-388S.

743 Yuan, G., Wahlqvist, M., Guoqing, H., Yang, M., Duo, L., 2006. Natural products
744 and anti-inflammatory activity. Asia Pacific journal of clinical nutrition 15, 143-
745 152.
746 Zhang, Q., Zhang, J. , Shen, J., Silva, A., Dennis, D., Barrow, C., 2006. A simple
747 96-well microplate method for estimation of total polyphenolic content in
748 seaweeds. Journal of Applied Phycology 18, 445-450.
749

750

Table 1(on next page)

Table [1]: Compounds identified from the total leaf extract of *Schotia brachypetalea*, its fractions and subfractions

#	Compound	Class	t_R (min.)	[M-H]$^-$ (*m/z*)	MS/MS fragment	Reference	Source (t_R min.)				
							Extract *(peak area %)*	**Fr.3**	**Fr.4**	**Sub. 1**	**Sub. 2**
1	Daidzein	Isoflavone	1.68	253	253	(Hanganu, Vlase & Olah, 2010)	√ *(1.32%)*	-	-	-	-
2	Digalloyl quinic acid	Gallotannin	11.56	495	343	(Sannomiya, Montoro& Piacent, 2005)	√ *(1.32%)*	√ (24.27)	√ (10.92)	√ (12.28)	√ (11.46)
3	Narirutin (naringenin-7-*O*-rutinoside)	Flavonoid glycoside	18.5	579	433, 271	(Sanchez-Rabaneda et al., 2004)	√ *(1.32%)*	√ (18.35)	-	-	
4	Digalloyl quinic acid	Gallotannin	24.48	495	343	(Sannomiya, Montoro& Piacent, 2005)	√ *(1.25%)*	-	√ (12.47)	-	-
5	Digalloyl hexose	Hydrolysable tannin	29.12	483	343	(Poay, Kiong & Hock, 2011)	√ *(1.20%)*	√ (17.12)	√ (29.13)	√ (15.62)	-
6	Myrecitin-3-*O*-(2"-*O*-galloyl)-hexoside	Galloylated flavonoid glycoside	39.92	631	479, 317	(Saldanha, Vilegas& Dokkedal, 2013)	√ *(2.36%)*	√ (38.84)	√ (48.93)	-	-
7	Myrecitin-3-*O*-(2"-	Galloylated	40.05	631	479, 317	Saldanha,	√	√	-	-	-

	O-galloyl)-hexoside	flavonoid glycoside				Vilegas& Dokkedal, 2013)	*(3.98%)*	(39.35)			
8	Quercetin-3-*O*-glucouronide	Flavonoid	43.62	477	301, 179, 151	(Saldanha, Vilegas& Dokkedal, 2013)	√ *(4.85%)*	√ (42.80)	√ (43.36)	-	√ (31.21)
9	Quercetin-3- *O*-(2"-*O*-galloyl)-hexoside	Galloylated flavonoid glycoside	44.03	615	463, 301	(Saldanha, Vilegas& Dokkedal, 2013)	√ *(12.81%)*	√ (44.72)	√ (47.64)	-	-
10	Quercetin-3- *O*-(2"-*O*-galloyl)-hexoside	Galloylated flavonoid glycoside	46.76	615	463, 301	(Saldanha, Vilegas& Dokkedal, 2013)	√ *(15.75%)*	√ (45.05)	√ (52.41)	-	-
11	Quercetin-hexose-protocatechuic acid	Galloylated flavonoid glycoside	51.48	599	463, 300	(Abdel-Hameed, Bazaid & Salman, 2013)	√ *(7.34%)*	√ (50.76)	√ (65.20)	-	-
12	Quercetin-hexose protocatechuic acid	Galloylated flavonoid glycoside	54.71	599	463, 300	(Abdel-Hameed, Bazaid & Salman, 2013)	√ *(5.62%)*	√ (51.13)	√ (65.28)	-	-
13	Quercetin-3-*O*-rhamnoside	Flavonoid glycoside	57.01	447	301	(Saldanha, Vilegas& Dokkedal,	√ *(5.72%)*	√ (56.17)	-	-	√ (58.78)

						2013)					
14	Myricetin-3-*O*-α-arabinopentoside	Flavonoid glycoside	59.91	449	271, 179	(Saldanha, Vilegas& Dokkedal, 2013)	√ *(2.56%)*	-	-	-	-
15	Kaempferol-3-*O*-rhamnoside	Flavonoid glycoside	63.56	431	285	(Diantini, Subarnas, & Lestari, 2012)	√ *(2.75%)*	-	-	-	-
16	Kaempferol derivative	Flavonoid glycoside	68.61	583	285	(Saldanha, Vilegas& Dokkedal, 2013)	√ *(1.29%)*	-	-	-	-
17	Myricetin-3-*O*-α-arabinopentoside	Flavonoid glycoside	69.70	449	271, 179	(Saldanha, Vilegas& Dokkedal, 2013)	√ *(4.94%)*	-	-	-	-
18	Unidentified	------	7.1	611	------	------	-	√	-	-	-
19	Pentagalloyl-hexoside	Hydrolysable tannin	11.2	991	495, 343	(Poay, Kiong & Hock, 2011)	-	√	-	-	-
20	Trigalloyl hexose isomer	Hydrolysable tannin	33.68	635	463,343,211, 161	(Poay, Kiong & Hock, 2011)	-	-	√	√	-
21	1-*O*-galloyl-6-*O*-cinnamoyl-*p*-	Hydrolysable tannin	33.3	607	461	Tentative	-	√	-	-	-

	coumaryl-hexoside										
22	Luteolin-7-*O*-6”-acetylhexoside	Flavonoid	40.10	489	467,285	(Saldanha, Vilegas& Dokkedal, 2013)	-	√	-	-	-
23	Caffeoyl-*O*-hexo-galloyl	Hydrolysable tannin	43.62	493	331,313	(Poay, Kiong & Hock, 2011)	-	√	-	-	-
24	Procyanidin trimer	Procyanidin	60.88	850	697, 425, 407	(Poay, Kiong & Hock, 2011)	-	√	-	√ (60.76)	-
25	Methoxylated castalagin/vescalagin	Methyl flavonoid glycoside	64.75	963	933	(Rauha, Wolfender &Salminen, 2001).	-	√	-	√ (64.67)	√ (64.65)
26	Myrecitin-3-*O*-(2"-*O*-galloyl)-pentoside	Galloylated flavonoid	65.07	601	449	(Saldanha, Vilegas& Dokkedal, 2013)	-	√	-	-	-
27	Myrecitin-3-*O*-(2"-*O*-galloyl)-pentoside	Galloylated flavonoid	66.02	601	449	(Saldanha, Vilegas& Dokkedal, 2013)	-	√	-	-	-
28	Quercetin-3-*O*-(2"-*O*-galloyl)-pentoside	Galloylated flavonoid	67.38	585	433, 301	(Saldanha, Vilegas& Dokkedal, 2013)	-	√	-	-	-

29	Luteolin aglycone	Flavonoid	67.45	285	285	(Saldanha, Vilegas& Dokkedal, 2013)	-	√	-	-	-
30	Isorhamnetin	Flavonol	67.68	315	301, 151	(Rabaneda *et al.*,2003)	-	√	-	√ (75.88)	-
31	(epi) Catechin gallate	Flavanol	2.58	441	289, 169, 135	(Bastos *et al.*, 2007)	-	-	-	√	√ (2.58)
32	Galloyl quinic acid/epiquinic	Hydroxybenzoic acid derivative	4.86	343	191, 85	(Clifford, Stoupi & Kuhnert, 2007)	-	-	-	√	-
33	Galloyl quinic acid /epiquinic	Hydroxybenzoic acid derivative	6.49	343	191, 85	(Clifford, Stoupi & Kuhnert, 2007)	-	-	-	√	-
34	Dihydromyricetin methylated dihexoside derivative	Flavonoid dervitative	31.14	509	347	Tentative	-	-	-	√	-
35	Luteolin-7-*O*-hexosyl-8-*C*-(6"-acetyl)-hexoside	Acetyl flavonoid glycoside	37.77	651	489, 327 179,151	(Simirgiotis *et al.*, 2013)	-	-	-	√	-
36	Isorhamnetin acetyl	Acetylated	45.36	519	357,315	(Simirgiotis	-	-	-	√	√

	glucoside	flavonoid glycoside				*et al*., 2013)					(41.71)
37	Quercetin-3-*O*-hexoside	Flavonoid glycoside	48.87	463	301	(Sannomiya, Montoro& Piacent, 2005)	-	-	-	√	-
38	Quercetin-3-*O*-hexohexoside	Flavonoid glycoside	51.93	463	301	(Sannomiya, Montoro& Piacent, 2005)	-	-	-	√	-
39	Unidentified	----------	53.44	629	--------	---------	-	-	-	√	-
40	Kaempferol-3-*O*-rutinoside	Flavonoid glycoside	66.78	593	285	(Sannomiya, Montoro& Piacent, 2005)	-	-	-	√	
41	Luteolin-5-*O*-hexosyl-8-*C*-(6"-acetyl)-hexoside derivative	Acetyl flavonoid glycoside	6.35	687	651, 489, 327	(Simirgiotis *et al*., 2013)	-	-	-	-	√
42	Phloretin xyloglucoside	Dihydrochalcone	21.48	567	435, 273	(Balázs *et al*., 2012)	-	-	-	-	√
43	Procyanidin Dimer-hexoside	Flavonoid glycoside	55.78	737	611,449	(Balázs *et al*., 2012)	-	-	-	-	√

44	Tricin-7-*O*-neohesperidoside	*O*-methylated flavone	59.33	638	492,330	(Balázs *et al*., 2012)	-	-	-	-	√
45	Hesperitin	aglycone	63.44	301	157	(Balázs *et al*., 2012)	-	-	-	-	√

1

i

2

Table 2(on next page)

Table [2]: *In vitro* antioxidant activity of SBE

Table [2]: *In vitro* antioxidant activity of SBE

*** EC50= µg/ml, ** Fe^{2+} equivalents/mg of sample, *** Trolox equivalents/mg of sample**

	DPPH*	FRAP**	ABTS***
SBE	9	5000	1054
EGCG	3	25000	5293

1

Figure 1(on next page)

Negative LC/ESI/mass spectrum of phenolics from hydro-alcoholic extract of Schotia brachypetalea

Figure (1): Negative LC/ESI/mass spectrum of phenolics from hydro-alcoholic extract of Schotia brachypetalea

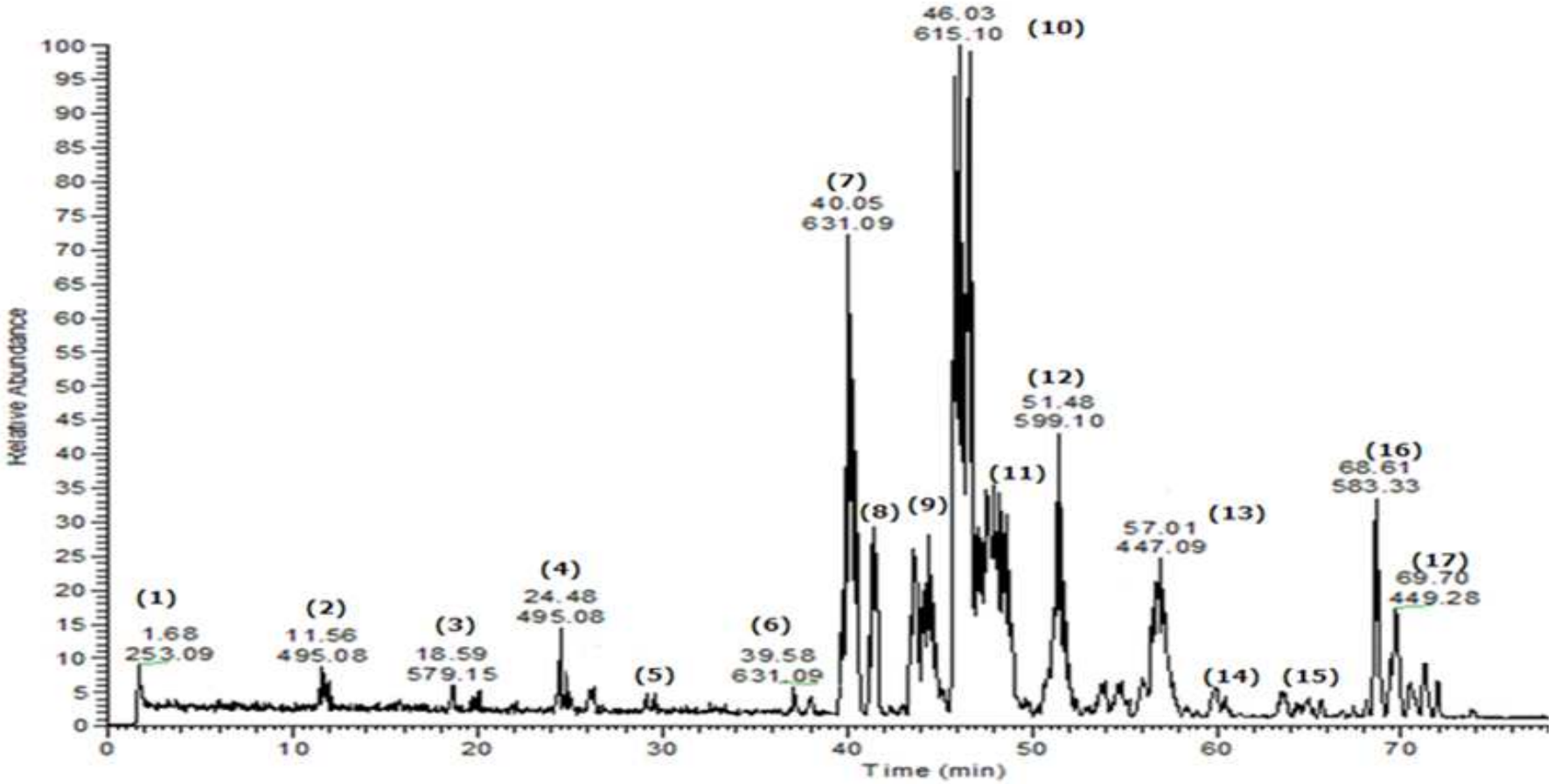

PeerJ PrePrints | https://doi.org/10.7287/peerj.preprints.1768v1 | CC-BY 4.0 Open Access | rec: 21 Feb 2016, publ: 21 Feb 2016

Figure 2(on next page)

Negative LC/ESI/mass spectrum of phenolics from fraction III of hydro-alcoholic extractof *Schotia brachypetalea*

Figure (2): Negative LC/ESI/mass spectrum of phenolics from fraction III of hydro-alcoholic extractof *Schotia brachypetalea*

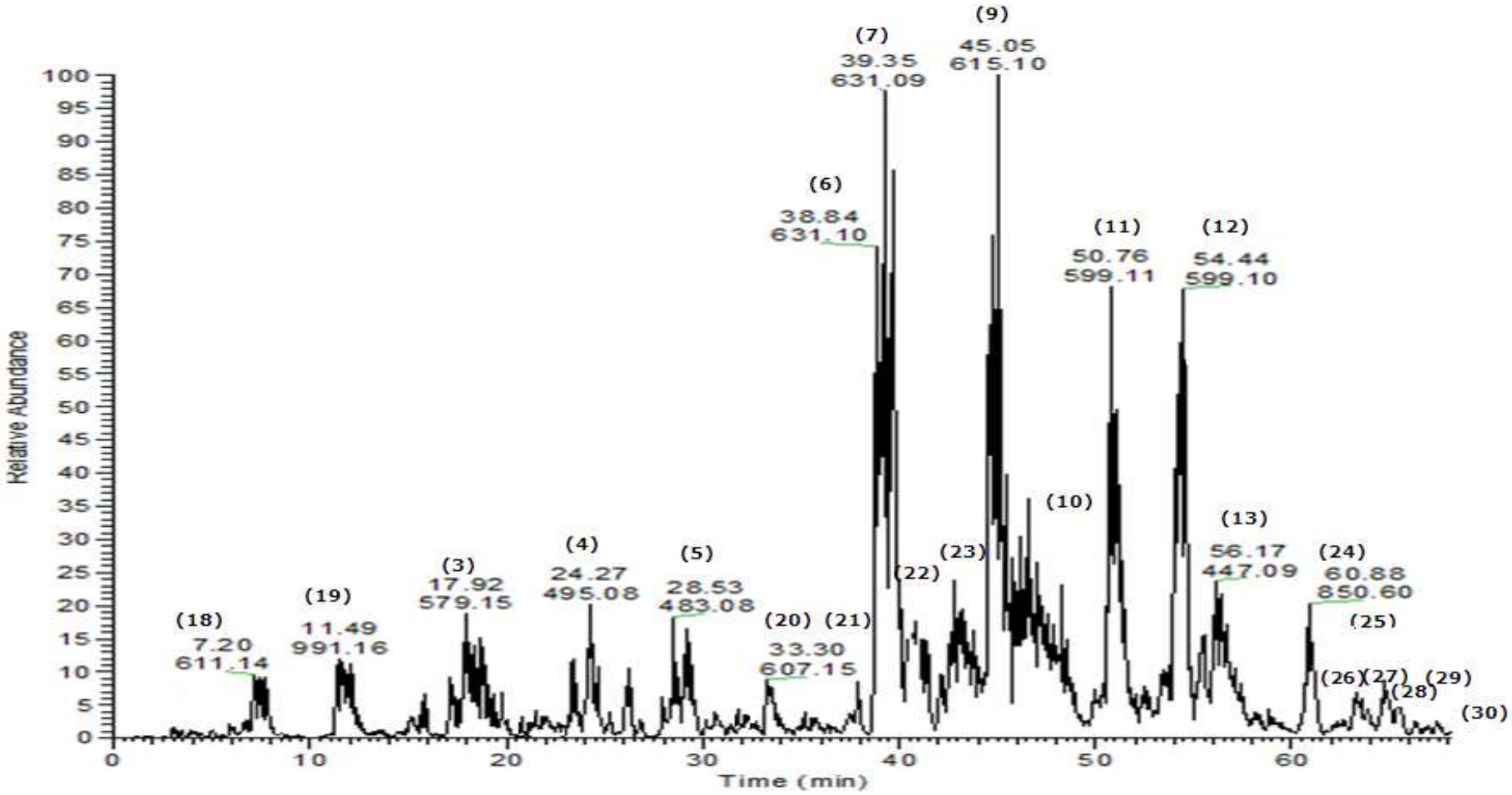

PeerJ PrePrints | https://doi.org/10.7287/peerj.preprints.1768v1 | CC-BY 4.0 Open Access | rec: 21 Feb 2016, publ: 21 Feb 2016

Figure 3(on next page)

Negative LC/ESI/mass spectrum of phenolics from fraction IV of hydro-alcoholic extractof *Schotia brachypetalea*

Figure (3): Negative LC/ESI/mass spectrum of phenolics from fraction IV of hydro-alcoholic extractof *Schotia brachypetalea*

PeerJ PrePrints | https://doi.org/10.7287/peerj.preprints.1768v1 | CC-BY 4.0 Open Access | rec: 21 Feb 2016, publ: 21 Feb 2016

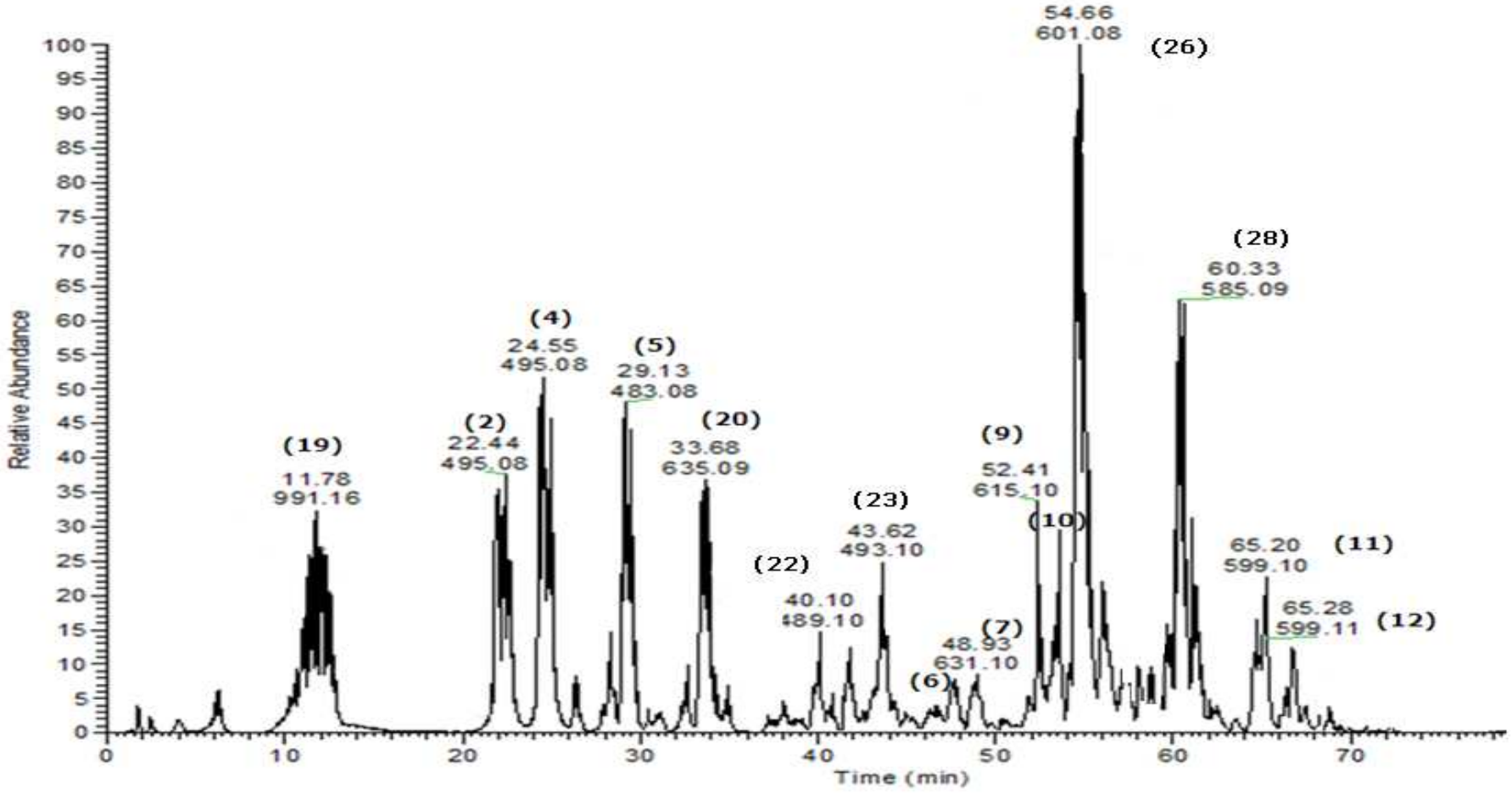

PeerJ PrePrints | https://doi.org/10.7287/peerj.preprints.1768v1 | CC-BY 4.0 Open Access | rec: 21 Feb 2016, publ: 21 Feb 2016

Figure 4(on next page)

Negative LC/ESI/mass spectrum of phenolics from Sub-fraction I (of fraction 4) of hydro-alcoholic extract of *Schotia brachypetalea*

Figure (4): Negative LC/ESI/mass spectrum of phenolics from Sub-fraction I (of fraction 4) of hydro-alcoholic extract of *Schotia brachypetalea*

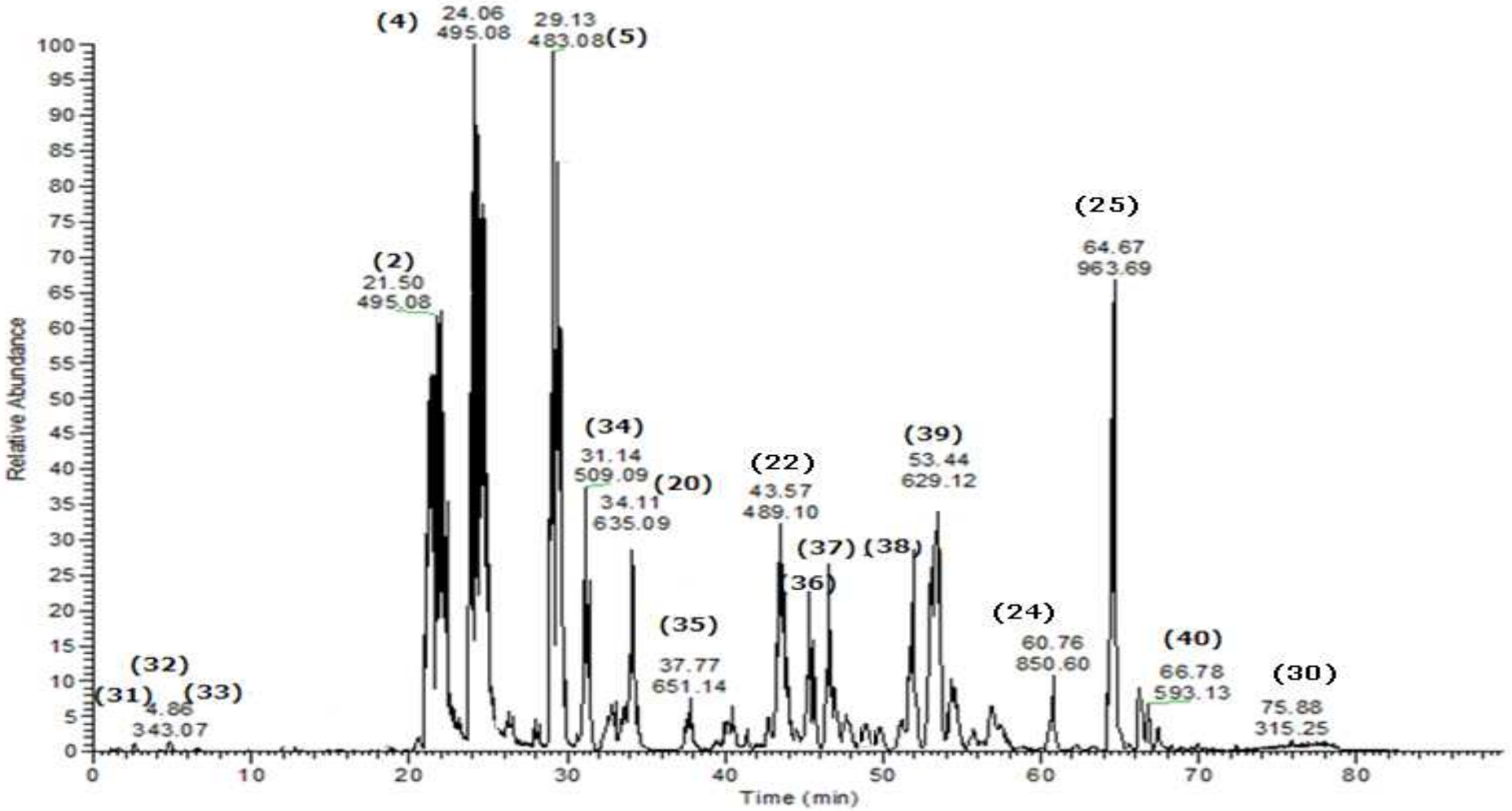

Figure 5(on next page)

Negative LC/ESI/mass spectrum of phenolics from Sub-fraction II (of fraction 4) of hydro-alcoholic extractof *Schotia brachypetalea*

Figure (5): Negative LC/ESI/mass spectrum of phenolics from Sub-fraction II (of fraction 4) of hydro-alcoholic extractof *Schotia brachypetalea*

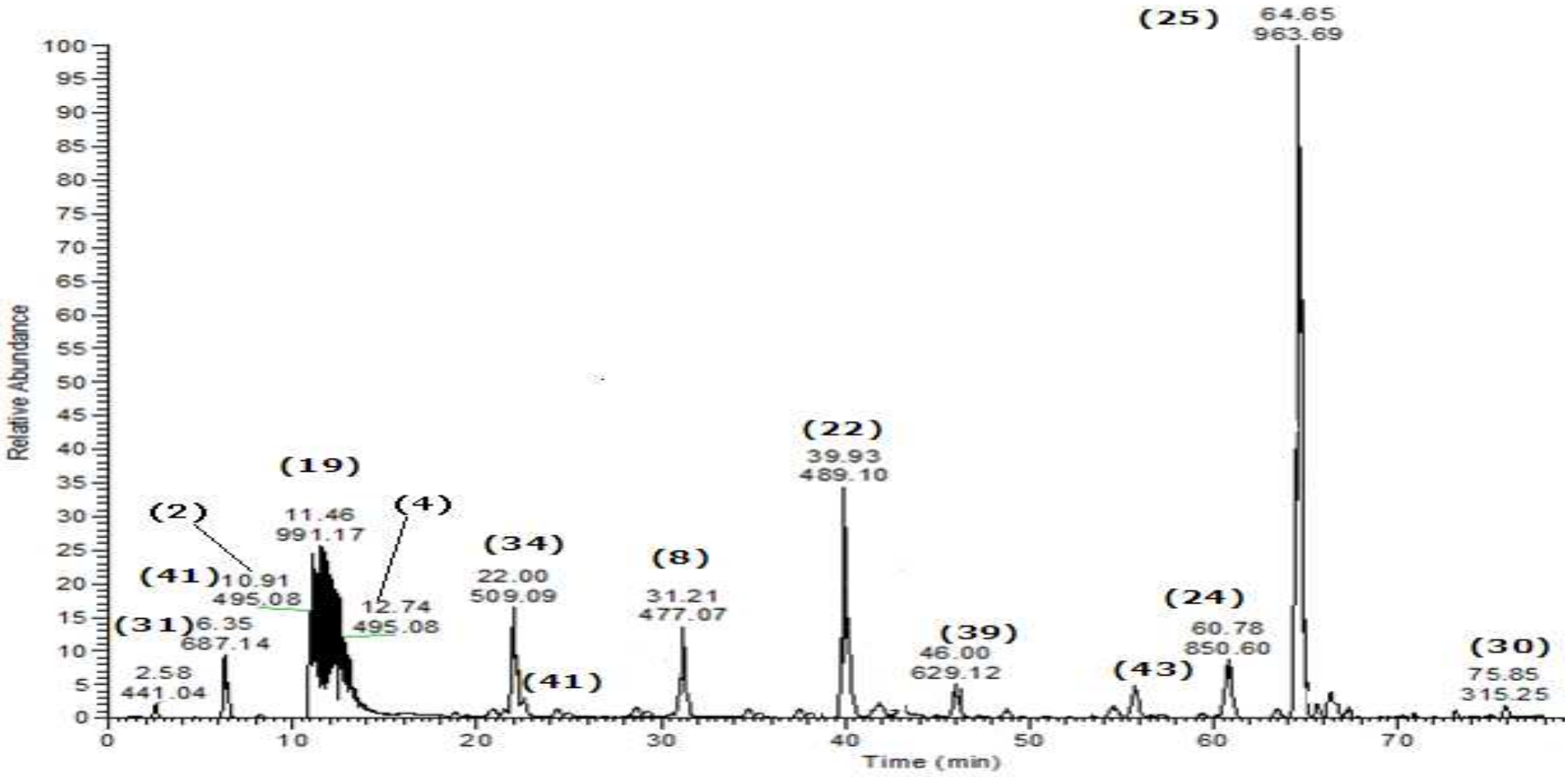

Figure 6(on next page)

Stress resistance of *C. elegans* under juglone treatment. Survival rates were significantly increased after pre-treatment of the nematodes with SBE. Data are presented as percentage of survivals (mean ± SEM, n=3). ** $p < 0.01$ and *** $p<0.001$ related

Figure (6): Stress resistance of *C. elegans* under juglone treatment. Survival rates were significantly increased after pre-treatment of the nematodes with SBE. Data are presented as percentage of survivals (mean ± SEM, n=3). ** $p < 0.01$ and *** $p<0.001$ related to the control by a one-way ANOVA followed by Bonferroni (post-hoc) correction.

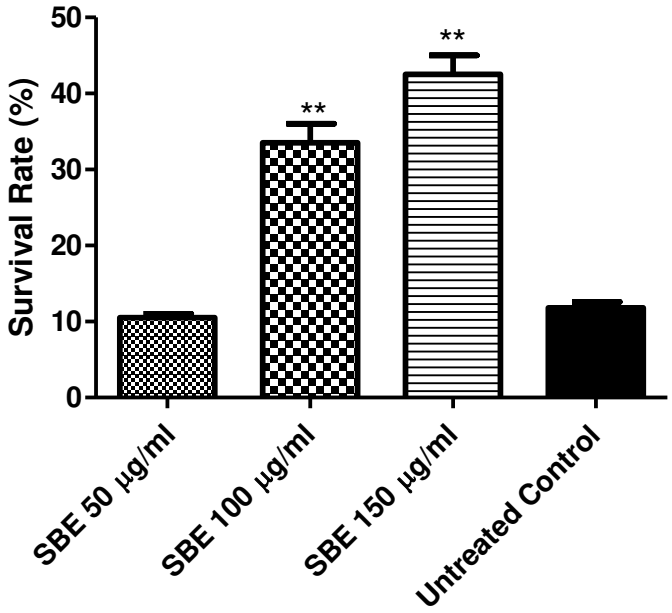

Figure 7 (on next page)

Effect of SBE on intracellular ROS accumulation in C. elegans. Data are presented as pixel intensity ± SEM (n=40, replicated 3 times). *** $p < 0.001$ related to the control by a one-way ANOVA followed by Bonferroni (post-hoc) correction. Micrographs show a

Figure (7): Effect of SBE on intracellular ROS accumulation in C. elegans. Data are presented as pixel intensity ± SEM (n=40, replicated 3 times). *** $p < 0.001$ related to the control by a one-way ANOVA followed by Bonferroni (post-hoc) correction. Micrographs show a representative worm treated with 50 µg SBE/ml (B), 100 µg SBE/ml (C), 150 µg SBE/ml (D) and a representative worm from the control group (E).

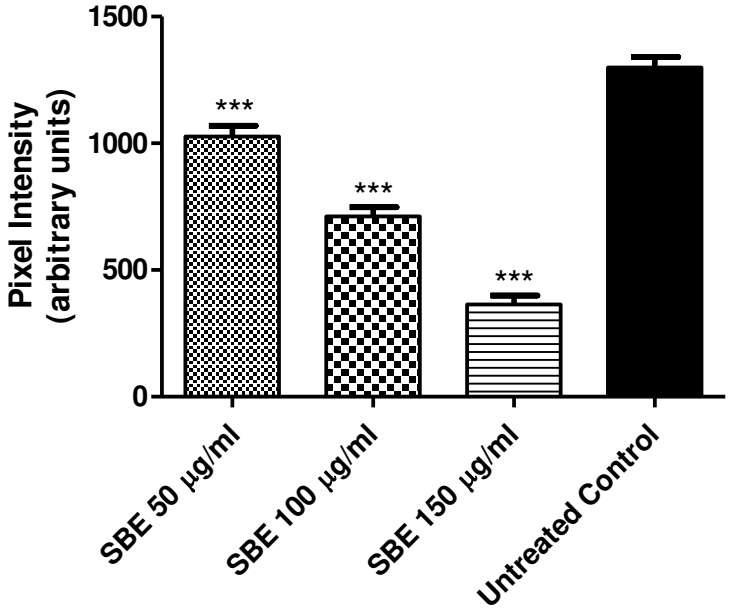

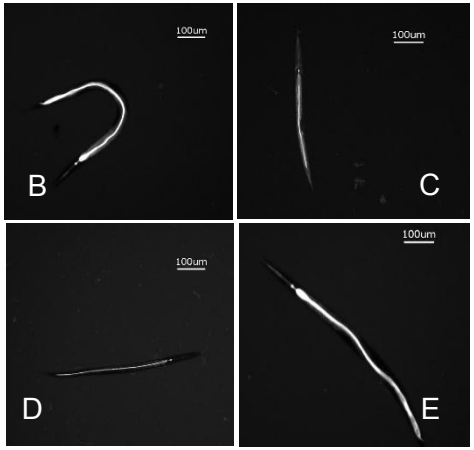

PeerJ PrePrints | https://doi.org/10.7287/peerj.preprints.1768v1 | CC-BY 4.0 Open Access | rec: 21 Feb 2016, publ: 21 Feb 2016

Figure 8(on next page)

Influence of SBE on hsp16.2::GFP expression in the transgenic C. elegans strain (TJ375 hsp-16.2::GFP(gplsI) under juglone-induced oxidative stress. Data are presented as pixel intensity (mean ± SEM, n=40, replicated 3 times). * $p < 0.05$ and *** $p < 0.001$

Figure (8): Influence of SBE on hsp16.2::GFP expression in the transgenic C. elegans strain (TJ375 hsp-16.2::GFP(gplsI) under juglone-induced oxidative stress. Data are presented as pixel intensity (mean ± SEM, n=40, replicated 3 times). * $p < 0.05$ and *** $p < 0.001$ related to the control, analysed by one-way ANOVA followed by Bonferroni (post-hoc) correction. Micrographs show a representative worm treated with three different concentrations 50 µg SBE/ml (B), 100 µg SBE/ml (C), 150 µg SBE/ml (D) and a representative worm from the control group (E).

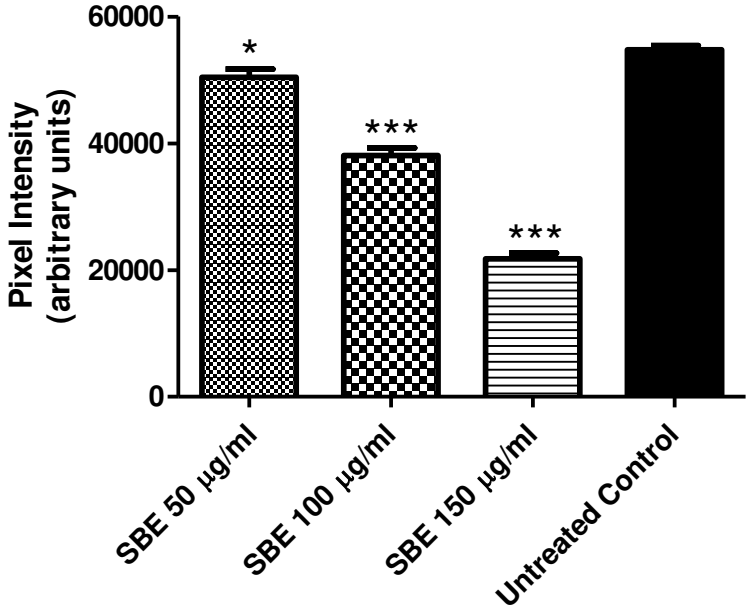

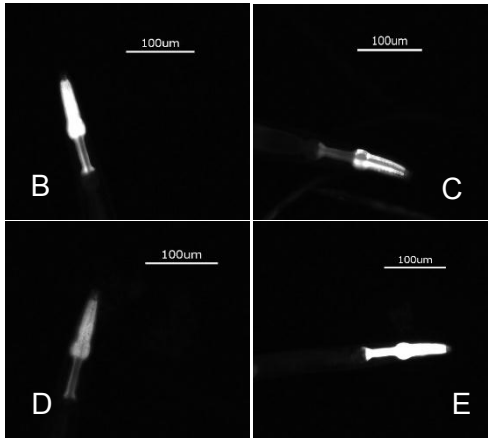

PeerJ PrePrints | https://doi.org/10.7287/peerj.preprints.1768v1 | CC-BY 4.0 Open Access | rec: 21 Feb 2016, publ: 21 Feb 2016

Figure 9(on next page)

Effect of the leaf extract from *S. brachypetala* (SBE) on DAF-16 subcellular pattern of location in the transgenic *C. elegans* strain (TJ356). Data show the percentage of worms exhibiting cytosolic, intermediate or nuclear pattern of location (A

Figure (9): Effect of the leaf extract from *S. brachypetala* (SBE) on DAF-16 subcellular pattern of location in the transgenic *C. elegans* strain (TJ356). Data show the percentage of worms exhibiting cytosolic, intermediate or nuclear pattern of location (A). *** $p < 0.001$ related to the control, analysed by one-way ANOVA followed by Bonferroni (post-hoc) correction. Micrographs illustrate representative location of DAF-16 in the cytosol (B), in cytosol and nucleus(C) and only in the nucleus (D).